

3D Monte Carlo Simulation of Phase Separation Kinetics in a Binary Metallic Alloy with Vacancy Mediated Diffusion: Effect of Initial Supersaturation

A. S. Shirinyan^a, Yu. S. Bilogorodskyy

Department of Physics, Cherkasy B. Khmelnytsky National University,
81, Shevchenko Street, Cherkasy, 18031, Ukraine
^ashirinyan@phys.cdu.edu.ua, aramshirinyan@ukr.net

Keywords: Monte-Carlo simulation, nucleation, separation kinetics, distribution function, stages.

Abstract. The process of phase formation at the initial stage of the reaction diffusion and growth of a new phase particles - at the atomic level by applying the Monte-Carlo simulation of the crystalline nanoalloy is presented. The influence of initial composition on the kinetics of phase separation in a binary alloy with the fcc crystal lattice has been analyzed in detail. The dependences of various parameters of tire process - the average size of new-phase particles, volume of new-phase clusters, size distribution function, dispersion and supersaturation - on time have been calculated. The obtained results demonstrate the opportunity of a three-stage separation process at low initial supersaturation values and a two-stage separation at large initial supersaturation values.

1. Introduction

The greatest progress that was achieved during last decade in materials science research is related to the creation of micro- and nanostructured materials operational characteristics which was determined at a microscopic level. Then it is obvious that macroscopic results should be considered at a microscopic level.

In a macroscopic bulk system, the first order phase transition occurs through the nucleation and the growth of particles of a new phase. Four consecutive stages are distinguished: 1) the nucleation, 2) the stage of independent growth of particles of a new phase, 3) the intermediate stage, and 4) coalescence (or the so-called Oswald ripening stage).

The final stage of phase transition is described by the Lifshits-Slezov-Wagner theory of coalescence. Coalescence is calculated only in the mean-field approximation and for infinitesimally small initial supersaturations, while the volume of the alloy is supposed to be infinitely large [1]. One might expect the volume fraction of new phase particles to influence the coarsening process and whole kinetics as well. Also, the problem of the initial stages description remains unresolved.

One of the promising methods in this respect is the computer simulation of the above phenomenon which allows obtaining the sufficient statistics (about 10^6 atoms to be collected) and investigating the evolution of all parameters in detail.

In this work we attempted to describe the process of phase formation at all stages of the reaction diffusion - at the atomic level by applying the three-dimensional (3D) computer simulation of the crystalline alloy (figure 1). Time method applied for studying the kinetics of the system relaxation was the method of Monte-Carlo computer simulation of the vacancy diffusion. We have constructed a kinetic Monte-Carlo model for the phase decomposition in a binary system with the fcc lattice and analyzed the alloy separation at every evolution stage of the system concerned.

The paper is structured as follows. In the next section we describe the basic assumptions of MC method for the microscopic theory of diffusion and present the three-dimensional MC model of separating alloy. In section 3, we investigate the kinetics of the decomposition related to the influence of supersaturation. Concluding remarks are given in section 4.

2. Model

Let us apply the fundamental concepts of the diffusion microscopic theory to alloys and select the most probable diffusion mechanism for metallic alloys. Usually the diffusion in the mixture consisting of two sorts of atoms is modelled by Kawasaki direct exchange dynamics. This is not a satisfactory representation of the diffusion in real alloys, where atoms can change places easily due to empty neighboring site [2-3]. In the present communication, we study the process of vacancy-mediated phase separation in a system consisting of atoms of two different types, A and B, and describe the corresponding evolution of the process. In this instance we treat the case of a binary metallic alloy $A_{1-C}B_C$ with the initial composition C_0 as a supersaturated system whereas a nucleus of a new phase will have another stoichiometry $C_n=1$ (pure B atoms).

In order to calculate the configurational energy of the system, in which atoms were located at the lattice points, we used the Ising Hamiltonian, which took into account the energies of pair interatomic interactions only within the limits of the first coordination sphere [4]. A single vacancy was introduced into a spatial specimen with the fcc symmetry; the energy of interaction between this vacancy and other atoms was supposed to be equal to zero. The pair interaction potential Φ_{XY} , where the subscripts X and Y can possess one of the values: A (for A atoms), B (for B atoms), or V (for vacancies), was assigned to each pair of the particles. In this case, the configurational energy of the whole system looks like

$$E = \frac{1}{2} \sum_{i=1}^{N_0} \sum_{j=1}^Z \Phi_{X_i Y_j}, \quad (1)$$

where the external summation is carried out over all N_0 lattice points of the system, while the internal one is realized only over the points within the first coordination sphere of the i -th lattice point.

Consider basic model of the vacancy-mediated diffusion. The activation energy for the diffusion hop, Q , is evaluated as follows. Let us assume (figure 2) that the energies of the initial and end positions of the atom in the lattice are different, while the barrier height E_0 in the crossover point of potential energy relief is the same for all atoms [5]. The depth of the well, where the atom is located, depends on the atom's nearest environment, that is the value E_i for the i -th atom can be determined within the first coordination sphere by Ising-type model:

$$E_i = \sum_{j=1}^Z \Phi_{X_i Y_j}. \quad (2)$$

$Z=12$ is the number of the vacancy's nearest-neighbour atoms. The value of the activation energy Q for the microscopic diffusion of the X type atom (here $X = A, B$), moving from point 1 to point 2 (figure 2), is given by the quantity: $Q=E_0-E_1$. In general, if the i -th atom adjoins the vacancy, activation energy barrier height for the diffusion jump of the vacancy towards i -th direction is expressed by:

$$Q_i = E_0 - E_i. \quad (3)$$

The residence time algorithm uses the 'forced' jump along the randomly selected i -direction. The probability of one diffusion jump along each direction is given by the ratio:

$$p_i = \frac{v_i}{\sum_{j=1}^Z v_j} = \frac{v_{0i} \cdot e^{\frac{-Q_i}{kT}}}{\sum_{j=1}^Z v_{0j} \cdot e^{\frac{-Q_j}{kT}}} = \frac{v_{0i} \cdot e^{\frac{E_i}{kT}}}{\sum_{j=1}^Z v_{0j} \cdot e^{\frac{E_j}{kT}}}. \quad (4)$$

Here v_i is the frequency of the atom-vacancy interchange in the i -th direction, j is the number adjacent to the vacancy atom. Having obtained the p_i values, one finds the successful jump

direction by randomly generating R and comparing it with the p_i , ν_{0i} is the vacancy- i -atom exchange characteristic frequency [2-3,6]. The probabilities are normalized to unity.

Therefore, the algorithm for simulating the vacancy diffusion is as follows:

(i) The initial configuration of atoms is selected. The concentration of atoms is C_0 , and they are rigidly fixed at the points of the regular fcc crystal lattice, being randomly distributed over the latter.

(ii) A vacancy is inserted (one of the fcc lattice points is designated as non-occupied).

(iii) For the given vacancy position, probabilities (4) are evaluated for all possible jumps by calculating energies (2). Afterwards, according to the found probabilities the direction of the jump is selected randomly, by generating a random number R , and the interchange of the vacancy and the atom is carried out.

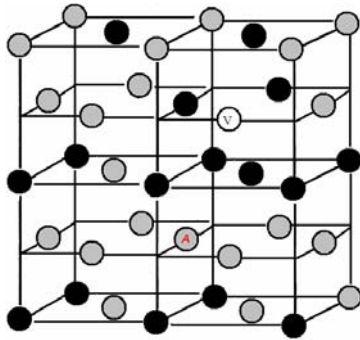


Fig. 1. Schematic representation of the fcc lattice: grey circles – atoms of one sort, black circles – atoms of the other sort. A single vacancy was introduced into a spatial specimen with the fcc structure (white circle).

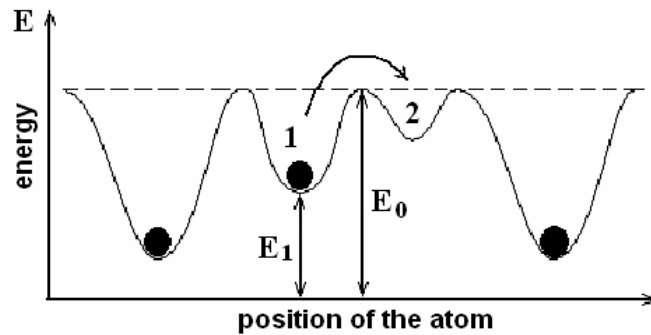


Fig. 2. Sketch-model of the barrier for the diffusion jump: for the atom jumping from position 1 into position 2. The activation energy Q , for 1→2 diffusion jump, is determined as the difference $E_0 - E_1$. The smaller the value E_1 is the larger the energy barrier $Q = E_0 - E_1$ for the diffusion becomes.

The obtained results were used for plotting the dependence of the concentration on time and the distribution function of clusters over their dimension $f(r)$, i.e. the number of nuclei with the r size. The model allows finding the most important characteristics of the distribution function such as the average size (radius) $\langle r \rangle$ and the time-dependent number $N \equiv N(t)$ of the new phase clusters, the dispersion, the slope, and the peak sharpness of the size distribution function. The results obtained for the function $f(r)$ can also be compared in the space of average quantities, where the part of the parameter is played by the ratio between the new phase particle radius $r(t)$ and the average radius $\langle r \rangle$ rather than the radius r itself. Furthermore, the average volume of the particles in the new phase is determined by the formula: $\langle V \rangle = \sum_{n=1}^N N_n / N$, where N_n is the number of atoms in the n -th cluster ($n=1 \dots N$), and the size of the cluster r_n is defined as $r_n = \sqrt[3]{N_n}$, average size of the new formed phase then becomes $\langle r \rangle = \sum_{n=1}^N \sqrt[3]{N_n} / N$. This gives the opportunity to calculate the normalized dimension of the new phase $u_n = r_n / \langle r \rangle$ and the corresponding size distribution function $f(u_n) \equiv f(u)$. The total volume of the new phase is found by the formula: $V_{tot} = \sum_{n=1}^N N_n$ and the volume fraction of the new phase can be determined as $\rho = V_{tot} / N_0$. Dispersion D , slope Sk , and the peak sharpness Kr of the function $f(u)$ are determined by the formulas:

$$D = \sqrt{\frac{\sum_{n=1}^{N(t)} (u_n - 1)^2}{N(t)}}, \quad Sk = \frac{\sum_{n=1}^{N(t)} (u_n - 1)^3}{N(t)D^3}, \quad Kr = \frac{\sum_{n=1}^{N(t)} (u_n - 1)^4}{N(t)D^4} - 3. \quad (5)$$

Here $\bar{u} = 1$.

In the following analysis, only those particles, in which one atom B was surrounded by not less than $N_{\min}=10$ atoms of the same sort, were attributed to the new phase. Such a choice of the minimal number of surrounding atoms N_{\min} was relative. In our case, the given value for N_{\min} was caused by the alloy model with the fcc crystal lattice, where $Z=12$.

We also determine the supersaturation in the alloy during the phase separation process as the function of the MCS. For this purpose, we have to know the composition of B component outside the particles of the new phase, i.e. in that portion of the alloy, where there were no nuclei of the new phase. Hereinafter, we use the notation C for this composition.

3. Results and Discussion

Computer experiments were carried out for the fcc crystal lattice composed of 1 million atoms (the spatial analogs of the $100 \times 100 \times 100$ lattice). The periodic Born-Karman boundary conditions were applied along all the axes. The model parameters were the following: the temperature $T=300\text{K}$, the pair interaction energies $\Phi_{AA}=\Phi_{BB}=-2 \times 10^{-20}\text{J}$ and $\Phi_{AB}=-1.8 \times 10^{-20}\text{J}$ and the component jump frequencies - $\nu_{oA}=1 \times 10^{13}\text{Hz}$ and $\nu_{oB}=3 \times 10^{13}\text{Hz}$.

The obtained results demonstrate the essential variation of the $f(u)$ function behavior depending on the initial supersaturation value. As a matter of fact, the cases of low and high initial supersaturations C_0 may be conventionally distinguished. The detailed evolution of the distribution function $f(u)$ at all stages of decomposition is discussed in [5], where we've shown that in case of low initial supersaturation the size distribution function first quickly becomes exponential and, afterwards, bimodal and at least, at the final stage, the distribution function becomes unimodal one. At high initial supersaturation values, the behavior of the distribution function differs drastically. Namely, the distribution function remains unimodal, and its maximum moves towards larger dimensions [5].

In this communication we draw attention to the basic characteristics evolution, namely, D , $\langle r \rangle$, N , V_{tot} , E . We observe a three-stage decomposition process in a binary alloy at low initial supersaturation values (nucleation, slow growth, and coalescence) and a two-stage decomposition at large initial supersaturation values (first, the emergence and quick growth of the new phase occur simultaneously; afterwards, the slow coalescence and coagulation take place, simultaneously as well). The reduction of C_0 results in slowing down the whole process of phase separation (figures 3, 4 and insets).

Let us consider the process of decomposition in greater detail. Figure 4 demonstrates that the reduction of the initial supersaturation brought about the appearance of maxima in the evolution plots $N(t)$. The maximum point, corresponding to the maximal number of the new-phase particles, shifted towards larger times. The appearance of the maximum showed that the process of the new phase nucleation took place. At this stage we see nano-, meso- and macroparticles of the new phase. Then, depending on the value of the supersaturation C_0 , the whole process follows either through one subsequent stage (quick transition to the stage of coalescence and coagulation) or through two subsequent stages (quick transition to the growth, and coalescence).

For the description of the initial stage to be complete, the evolution of the distribution function dispersion for various values of C_0 is shown in figure 3. In accordance with the model, the phase separation began as the particle size dispersion increased. Again, we see that evolution of D depends on the initial supersaturation C_0 .

Such a scenario explains the change of the average radius with time for various initial concentrations (figure 5). Another characteristics, such as mean composition of the B component around the new formed nuclei, C , are shown in figure 6.

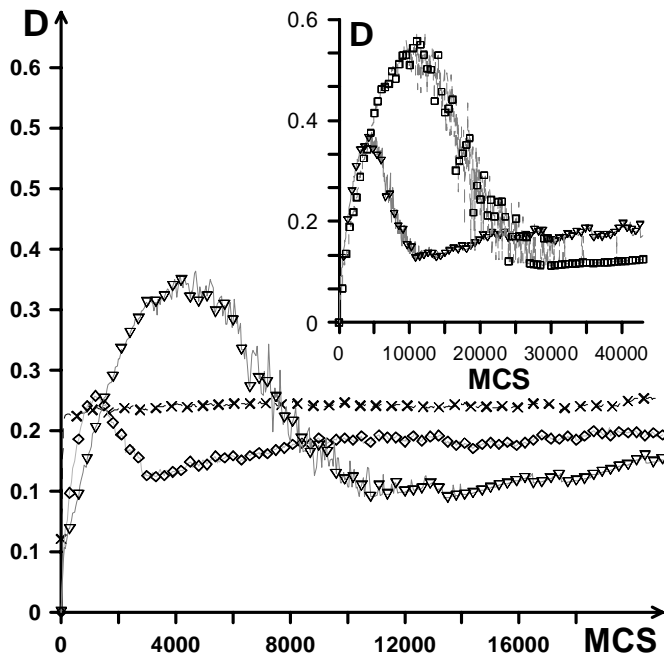


Fig. 3 The dispersion D as the function of the MCS number for various initial values of supersaturation: $C_0 = 0.1$ (x), $C_0 = 0.025$ (◇), $C_0 = 0.0175$ (▽), $C_0 = 0.015$ (□). Other parameters are the same and indicated in the text. Each point is averaged over 20 independent realizations.

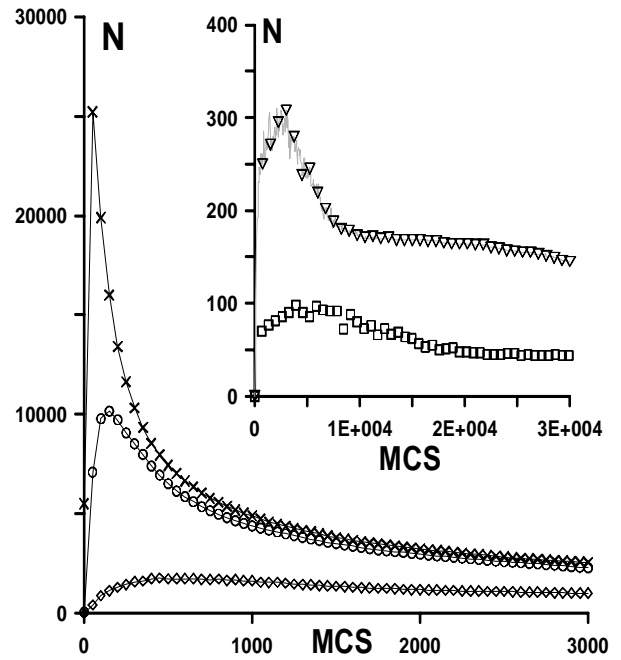


Fig. 4 Evolution of the clusters number $N(t)$ during the separation for different values of the initial composition C_0 : $C_0 = 0.1$ (x), $C_0 = 0.05$ (o), $C_0 = 0.025$ (◇), $C_0 = 0.0175$ (▽), $C_0 = 0.015$ (□). Each point is averaged over 20 realizations.

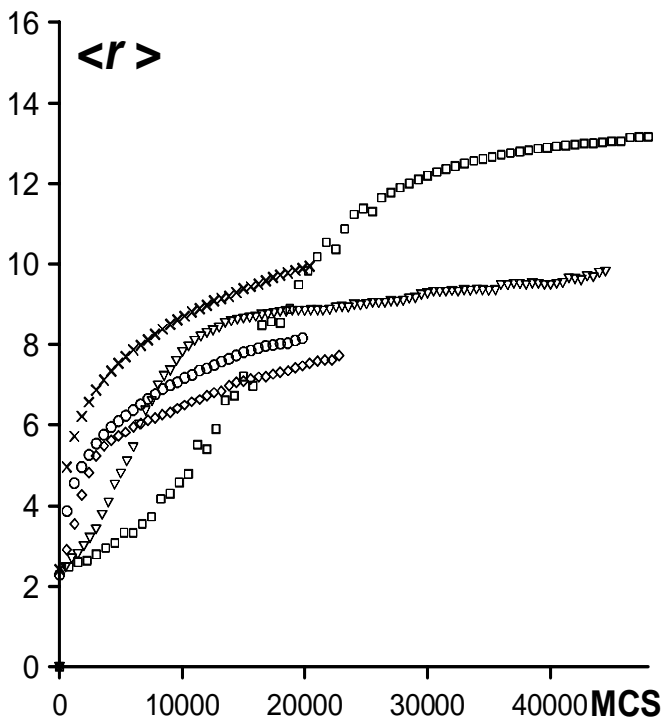


Fig. 5 Average size $\langle r \rangle$ versus MCS for different values of C_0 : $C_0 = 0.1$ (x), $C_0 = 0.05$ (o), $C_0 = 0.025$ (◇), $C_0 = 0.0175$ (▽), $C_0 = 0.015$ (□) while other parameters are the same. The simulations are averaged by 20 independent program starts.

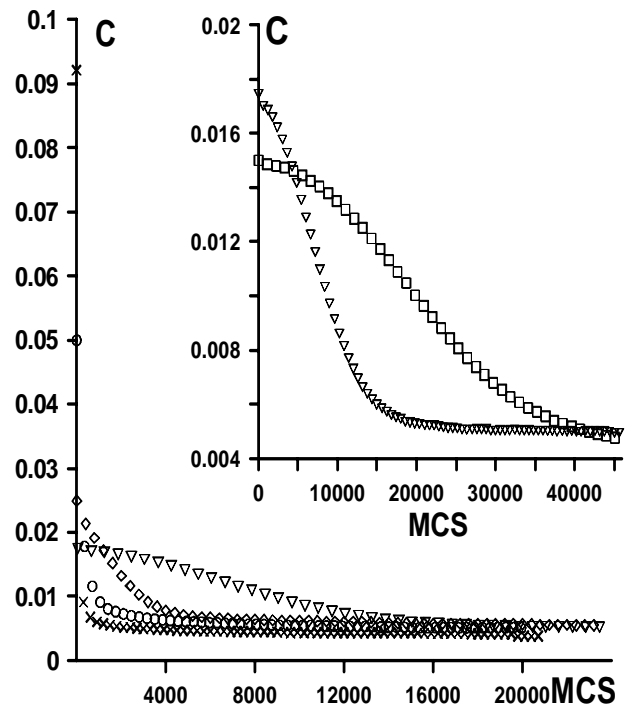


Fig. 6 Dependences of the concentration in the parent phase on time during the decomposition process: $C_0 = 0.1$ (x), $C_0 = 0.05$ (o), $C_0 = 0.025$ (◇), $C_0 = 0.0175$ (▽), $C_0 = 0.015$ (□). Each point is averaged over 20 realizations.

Figures 5-6 confirm our statement about the dependence of the decomposition stage number on the magnitude of the initial supersaturation. The results testify to the fact that the higher C_0 is, the faster the alloy relaxes to the equilibrium state and approaches the stage of coalescence and coagulation.

4. Summary and Concluding Remarks

The obtained results demonstrate the opportunity of a three-stage decomposition process in a binary alloy at low initial supersaturation values (nucleation, slow growth, and coalescence) and a two-stage decomposition at large initial supersaturation values (first, the appearance and the quick growth of the new phase occur simultaneously; afterwards, the slow coalescence and coagulation also take place simultaneously).

The results prove that the higher the initial supersaturation is, the faster the alloy relaxes to the equilibrium state and approaches the stage of coalescence and coagulation.

The new three-dimensional model based on another assumption of barrier for the diffusion jump (figure 2) was done by the authors in order to prove the scheme and results and in order to compare it with the real experimental observation and satisfactory explanation of diffusion effects. Results of the corresponding 3D model show the similar behaviour and will be discussed elsewhere.

Thus, the proposed approximation considerably improves our understanding of the mechanisms of nucleation and growth of the new-phase particles in a metastable system. The analysis carried out in this work is to be continued by the studies of the kinetics of the initial stages of the phase separation in a multicomponent alloy, provided several new phases can emerge. The corresponding simulation is being in progress now.

References

- [1] I. M. Lifshits, V. V. Slezov: *Fiz. Tverd. Tela* Vol. 1 (1959), p. 1401.
- [2] C. Castellano, F. Corberi: *Phys. Rev. B* Vol. 63 (2001), p. 060100.
- [3] P. Frantzl, O. Pentrose: *Phys. Rev. B* Vol. 50 (1994), p.3477.
- [4] Yi. Jiang, James A. Glazier: *Philosophical Magazine Letters* Vol. 74 (1996), p.119.
- [5] A. Shirinyan, Yu. Belogorodskyy: *Ukrainian Journal of Physics* Vol. 51 (2006), p. 605.
- [6] R. Kozubski , S. Czekaj , M. Kozłowski , E. Partyka, K. Zapala 9th International Symposium on Physics of Materials *ISPMA-9*, (Trans Tech Publications, Praha 2003).